VAPORIZATION OF LOW-VOLATILE FISSION PRODUCTS UNDER SEVERE CANDU REACTOR ACCIDENT CONDITIONS

B.J. Lewis, B.J. Corse, W.T. Thompson and M.H. Kaye
Royal Military College of Canada, Department of Chemistry and Chemical Engineering
PO Box 17000 Stn Forces, Kingston, Ontario, Canada K7K 7B4

F.C. Iglesias
Ontario Hydro, Reactor Safety and Operational Analysis Department
700 University Avenue, Toronto, Ontario, Canada M5G 1X6

P. Elder*, R. Dickson and Z. Liu
Atomic Energy of Canada Limited-Research Company, Chalk River Laboratories
Chalk River, Ontario, Canada K0J 1J0

ABSTRACT

An analytical model has been developed to describe the release behaviour of low-volatile fission products from uranium dioxide fuel under severe reactor accident conditions. The effect of the oxygen potential on the chemical form and volatility of fission products is determined by Gibbs-energy minimization. The release kinetics are calculated according to the rate-controlling step of diffusional transport in the fuel matrix or fission product vaporization from the fuel surface. The effect of fuel volatilization (i.e., matrix stripping) on the release behaviour is also considered. The model has been compared to data from an out-of-pile annealing experiment performed in steam at the Chalk River Laboratories.

1. INTRODUCTION

During a severe reactor accident, fission products (FPs) will be released from the degraded core. The release behaviour will depend on the various physical and chemical processes that occur in the fuel matrix and in the surrounding gaseous atmosphere. The release kinetics of the more volatile FPs have been shown to depend on a rate-limiting process of solid-state diffusion through the UO_2 fuel matrix.[1,2] On the other hand, the release of the low-volatile ones will more likely depend on the FP partial pressure,[3-7] which is dependent on the chemical form of the FP. The FP speciation will be influenced by the oxygen potential of the gas environment, the relative quantities of fuel-to-gas at the site of the reaction, temperature and total hydrostatic pressure. Release from the fuel matrix will also occur by "matrix stripping" for those FPs previously contained in the volatilized portion of the fuel that has undergone oxidation to UO_3.[8,9,10]

In this work, an analytical model is developed to describe the low-volatile fission-product release behaviour and fuel volatilization kinetics in accordance with equilibrium thermodynamics and mass transfer considerations.[4] Chemical equilibrium is assumed for the determination of the FP chemical form and partial pressure using a Gibbs-energy minimization technique based on the Facility for the Analysis of Chemical Thermodynamics (FACT).[11] The FACT database[12-15] has been supplemented with additional thermodynamic data on 150 chemical species following an extensive literature review.[5-7,16-21] A closed-form algorithm, based on a method of chemical potentials, is also developed to rapidly re-construct all partial compound pressures for the vaporization calculation.

The model has been developed for both CANDU and pressurized water reactor fuel types.[4,22] This paper will focus on the application of the model to CANDU fuel and provide a comparison of the model to data from a separate-effects experiment at the Chalk River Laboratories (CRL) using a fuel fragment from a spent CANDU fuel element.

---

*Present address: Atomic Energy Control Board, P.O. Box 1046, Station B, Ottawa, Canada K1P 5S9.

2. MODEL DEVELOPMENT

The release of fission products from the damaged fuel rod occurs as a multi-step process, consisting of: (i) transport through the fuel matrix and/or release due to volatilization of the fuel matrix, and (ii) fission-product vaporization into the gas stream flowing past the rod. The release kinetics are therefore controlled by the rate-limiting step. These mechanisms are described mathematically in the following sections.

2.1 Fission-product transport through the fuel matrix.

Fission-product transport in the uranium dioxide fuel matrix can be described by a generalized diffusional release process. The release fraction is given by:

$$F_d = N_d(\tau)/N_{go} \tag{1}$$

where $N_d(\tau)$ is the number of atoms which have diffused through the solid matrix and N_{go} is the original inventory in the fuel at time $t = 0$. The function $F_d(\tau)$ is given by a transformed Booth relation:[2,4]

$$F_d = \begin{cases} 6\sqrt{\dfrac{\tau}{\pi}} - 3\tau, & for\ \tau \leq 0.1, \\ 1 - \dfrac{6}{\pi^2}\exp\{-\pi^2\tau\}, & for\ \tau > 0.1. \end{cases} \tag{2}$$

The dimensionless variable τ is evaluated from the integral relation

$$\tau = \int_0^t D'(t)dt, \tag{3}$$

where $D' = D/a^2$, D is the diffusion coefficient (in m^2/s) and a is the grain radius (in m). Equation (3) accounts for a time-variable diffusivity that depends directly on the temperature T and on the stoichiometry deviation x in UO_{2+x} as the fuel is oxidized. The diffusion coefficient for the volatile cesium species is given by the composite expression:[2,23]

$$D(x,T) = \left[1 + F_{in}\frac{dT}{dt}\right]D_{in}\exp\left\{-\frac{Q_{in}}{RT}\right\} + x^2 D_{ox}\exp\left\{-\frac{Q_{ox}}{RT}\right\} \tag{4}$$

where $F_{in} = 178$ s/K, $D_{in} = 7.6 \times 10^{-10}$ m^2/s, $Q_{in} = 70$ kcal/mol, $D_{ox} = 2.22 \times 10^{-8}$ m^2/s, $Q_{ox} = 40.2$ kcal/mol. The diffusivity in Eq. (4) is an "effective" quantity. The first term accounts for intrinsic diffusion (including any augmented release during temperature ramps as a consequence of fuel cracking, and bubble precipitation and release), whereas the second term describes accelerated diffusion from fuel-matrix oxidation (due to enhanced uranium vacancy production).

For the evaluation of the diffusivity in Eq. (4), the fuel oxidation kinetics must be determined. The stoichiometry deviation x can be evaluated as a function of time according to the expression:[2]

$$dx/dt = -\alpha(S/V)[x - x_e(t)], \tag{5}$$

where $\alpha = 0.365\exp\{-23500/T\}$ (m/s) and S/V is the effective surface-to-volume ratio of the fuel (m^{-1}). This effective ratio is equal to ~3 times the geometrical one in order to account for surface roughness and microcracking of the fuel.[2] The equilibrium stoichiometry deviation, x_e, in Eq. (5) can be evaluated by equating the oxygen potential in the fuel to that in the atmosphere. The oxygen potential (in kJ/mol O_2) for hyperstoichiometric fuel (UO_{2+x}) can be calculated from the Blackburn thermochemical model:[24]

$$\Delta G_{O_2} = RT\ln(p_{O_2}) = RT\ln\left\{\left(x(2+x)/(1-x)\right)^2 k\right\} \tag{6}$$

where $\ln k = 108x^2 - 32700/T + 9.92$, R is the ideal gas constant ($= 8.314 \times 10^{-3}$ kJ mol^{-1} K^{-1}), T is the temperature (in K) and p_{O2} is the oxygen partial pressure (in atm). The oxygen potential for an ideal gas mixture in the atmosphere consisting of H_2O, H_2 (produced from the Zircaloy/steam reaction), O_2 and inert gas (due to the possible presence of air in the reactor channel) can be evaluated as:[25,26]

$$p_i / p_{tot} = \dot{n}_i / \sum_{j=1}^{N} \dot{n}_j \, , \tag{7}$$

where p_i is the partial pressure of component i, p_{tot} is the total pressure of all gases (atm), $\dot{n}_i$ is the instantaneous molar flow rate of component i, and N is the total number of component gases in the system. For the H_2O decomposition reaction:

$$H_2O \overset{K_{H_2O}}{\Leftrightarrow} H_2 + \tfrac{1}{2}O_2 \, , \tag{8}$$

the equilibrium constant, K_{H_2O}, is:[27]

$$K_{H_2O} = p_{H_2}\sqrt{p_{O_2}} / p_{H_2O} = \exp\{0.9794 \ln T - 1.1125 - 28820/T\}. \tag{9}$$

If the rate of H_2O dissociation required to maintain equilibrium is β, the molar flow rates after dissociation are:[25]

$$\dot{n}_{H_2O} = \dot{n}^o_{H_2O} - \beta, \dot{n}_{H_2} = \dot{n}^o_{H_2} + \beta, \dot{n}_{O_2} = \dot{n}^o_{O_2} + \beta / 2 \tag{10}$$

where the superscript "o" refers to the initial input gas quantities. Hence, the conditions for equilibrium can be described by combining Eqs. (7), (9) and (10):

$$K_{H_2O} = \frac{\dot{n}^o_{H_2} + \beta}{\dot{n}^o_{H_2O} - \beta} \times \sqrt{\frac{p_{tot}\left\{\dot{n}^o_{O_2} + \frac{1}{2}\beta\right\}}{\dot{n}^o_{H_2O} + \dot{n}^o_{H_2} + \dot{n}^o_{O_2} + \dot{n}^o_{inert} + \frac{1}{2}\beta}} \tag{11}$$

Equation (11) can be solved for β, and knowing the input molar flows, the partial pressures of the individual components are determined as follows:

$$\frac{p_{H_2}}{p_{tot}} = \frac{\dot{n}^o_{H_2} + \beta}{\sum_{j=1}^{N} n_j}, \quad \frac{p_{O_2}}{p_{tot}} = \frac{\dot{n}^o_{O_2} + \frac{1}{2}\beta}{\sum_{j=1}^{N} n_j}, \quad \frac{p_{H_2O}}{p_{tot}} = \frac{\dot{n}^o_{H_2O} - \beta}{\sum_{j=1}^{N} n_j}, \quad \frac{p_{inert}}{p_{tot}} = \frac{\dot{n}^o_{inert}}{\sum_{j=1}^{N} n_j}, \tag{12}$$

where $\sum_{j=1}^{N} n_j = \dot{n}^o_{H_2O} + \dot{n}^o_{H_2} + \dot{n}^o_{O_2} + \dot{n}^o_{inert} + \frac{1}{2}\beta$. This methodology can also be developed further to include the measurement of the oxygen content of the flowing gas mixture with the use of solid-state oxygen sensors at upstream and downstream locations of the fuel specimen.[25] Thus, equating the oxygen partial pressures in Eqs. (6) and (12), one can obtain x_e as a function of time for the changing atmospheric conditions. In turn, $x(t)$ can be evaluated with Eq. (5) for use in the diffusion coefficient of Eq. (4).

2.2 Fission-product release from fuel volatilization.

Fission-product release from the fuel matrix can also arise from a matrix-stripping process as a consequence of fuel volatilization. Fuel volatilization in oxidizing conditions can be described by the following reaction:[10]

$$UO_{2+x}(s) + \frac{(1-x)}{2}O_2 \leftrightarrow UO_3(g) \, . \tag{13}$$

The equilibrium partial pressure of UO_3 will depend on the exposure time:[10]

$$p_{UO_3}(t) = p_{O_2}^{\frac{1-x(t)}{2}} \exp\left\{-\frac{\Delta G_{(13)}(t)}{RT}\right\} \tag{14}$$

$$\Delta G_{(13)}(t) = \Delta G_f^o(UO_3(g)) - \Delta G_f^o(UO_2) - \tfrac{1}{2}\int_0^{x(t)} \Delta G_{O_2}\, dx. \tag{15}$$

The partial molar Gibbs energy of oxygen in UO_{2+x} can be integrated using the Blackburn thermochemical model in Eq. (6) such that:

$$\tfrac{1}{2}\int_0^{x} \Delta G_{O_2}\, dx = RT\left\{\ln\left(\frac{x^x(2+x)^{(2+x)}(1-x)^{(1-x)}}{4}\right) - \frac{x}{2}\left(\frac{32700}{T} - 7.92\right) + 18x^3\right\}. \tag{16}$$

In addition, the UO_2 and UO_3 formation energies (in kJ mol^{-1}) in Eq. (15) are given by:[28,29]

$$\Delta G_f(UO_3(g) - \Delta G_f(UO_2) = 253.33 - 0.09523T. \tag{17}$$

For the evaluation of Eq. (14), the oxygen partial pressure and instantaneous stoichiometry deviation $x(t)$ is determined in accordance with the analysis of Section 2.1.

The rate of volatilization of the fuel matrix is controlled by UO_3 mass transport through a boundary layer at the surface of the fuel. Thus, the fuel volatilization rate depends on the partial pressure of the UO_3 (Eq. (14)) and the mass transfer from the fuel surface into the carrier gas stream. From mass transfer theory, the volatilization rate R_{vol} (in molecule s^{-1}) from an exposed surface area S (m^2) is given by:[3,4,10,30]

$$R_{vol} = \frac{SN_A}{M_{UO_{2+x}}}\frac{dm}{dt} = SN_A k_m\left(\frac{p^s_{UO_3}}{p_{tot}} - \frac{p^\infty_{UO_3}}{p_{tot}}\right) \tag{18}$$

where N_A is Avogadro's number (= 6.022×10^{23} molecule mol^{-1}), $M_{UO_{2+x}}$ is the molecular weight of UO_{2+x} (kg mol^{-1}), dm/dt is the vaporization mass flux of UO_{2+x} (kg m^{-2} s^{-1}), k_m is the mass transfer coefficient (mol m^{-2} s^{-1}) (see Section 2.3.1), $p^s_{UO_3}$ is the equilibrium partial pressure of UO_3 at the fuel surface (Eq. (14)) and $p^\infty_{UO_3}$ is the UO_3 partial pressure in the bulk gas stream which is assumed to be negligible in most cases. The fraction of fission products released from the fuel matrix, assuming a constant fission-product distribution within the fuel, is simply given by the mass fraction of volatilized fuel material:

$$F_{vol} = \Delta m / m_o \tag{19}$$

where m_o is the initial mass of fuel (in kg) and Δm is the mass of volatilized UO_{2+x}:

$$\Delta m = \left(M_{UO_{2+x}} / N_A\right)\int_0^t R_{vol}\, dt. \tag{20}$$

The fission products released by matrix stripping are no longer available for diffusional transport in the fuel matrix. Hence, using Eqs. (1) and (19), mass conservation implies that the number of atoms which reach the fuel surface by either diffusion or matrix stripping (N_{fs}) are:

$$N_{fs} = \{(1 - F_{vol})F_d + F_{vol}\}N_{go}\,. \tag{21}$$

Equivalently, the combined release fraction (F_{fs}) for the two release processes from the matrix to the fuel surface is:

$$F_{fs} = N_{fs} / N_{go} = \{(1 - F_{vol})F_d + F_{vol}\}\,. \tag{22}$$

2.3 Fission-product vaporization.

The vaporization release of low-volatile fission products from the fuel depends on the partial pressure of the species and the mass transfer from the fuel surface into the carrier gas stream. Analogous to Eq. (18), the release rate (R_{iv}) (in atom/s) of a fission product species *i*, vaporized from an exposed fuel surface area *S* (in m^2) is:

$$R_{iv} = S\gamma_i N_A k_{im}(x_{is} - x_{i\infty}), \tag{23}$$

where k_{im} is the mass transfer coefficient (see Section 2.3.1) (mol m^{-2} s^{-1}), x_{is} is the mole fraction of fission product *i* at the surface of the fuel, $x_{i\infty}$ is the mole fraction of fission product *i* in the bulk gas stream, γ_i is the number of atoms per molecule of fission product *i*, and N_A is Avogadro's number (= 6.022×10^{23} mol^{-1}). The mole fraction of fission product at the surface of the fuel is

$$x_{is} = p_{iv} / p_{tot}, \tag{24}$$

where p_{iv} is the partial pressure (in atm) of the fission product *i* in the vapor phase (see Section 2.3.2), and p_{tot} is the total system pressure. For the small quantities of low-volatile fission products anticipated in the bulk stream, it can again be assumed that $x_{i\infty} \approx 0$.

The number of atoms of a given fission product which are released by vaporization from the fuel surface (N_r) is given by:

$$N_r = \int_0^t R_{iv}(t)dt, \tag{25}$$

thereby yielding a release fraction for vaporization (F_v) of:

$$F_v = N_r / N_{go} = \int_0^t R_{iv}(t)dt / N_{go}. \tag{26}$$

Finally, the overall release fraction (*F*) for a given fission product is taken as the smaller of the two release fractions for release to the fuel surface (F_{fs}) (Eq. (22)) versus vaporization from that surface (F_v) (Eq. (26)):[4]

$$F = \min(F_{fs}, F_v). \tag{27}$$

The smaller fractional release value indicates the rate-controlling step.[4]

If the fuel is surrounded by a Zircaloy cladding, some fission products can be chemically-trapped in the cladding until it becomes oxidized. For example, tellurium will be released when the clad is ~60% oxidized, while antimony will remain trapped until the oxidation process is complete.[4] The effect of fission-product trapping for these species can be empirically modelled as a reduced overall fractional release where the result of Eq. (27) is multiplied by the fraction ($1-\zeta$). Here ζ is a trapping fraction which can be correlated with the oxidation state of the cladding and the temperature as shown in Ref. 4.

2.3.1 Mass Transfer Coefficient.

The mass transfer coefficient can be evaluated for a given geometry based on a heat/mass transfer analogy. For example, in the case of a forced-convective flow around a cylindrical fuel specimen (in the laminar flow regime) (dropping the subscript *i*):[4]

$$k_m = 4c D_{AB} / d \tag{28}$$

where *c* is the molar concentration of gas around the fuel specimen (= $p_{tot}/(RT)$), D_{AB} is the binary diffusion coefficient of a FP (for the dominant chemical form) or UO_3 compound (*A*) in a carrier gas atmosphere (*B*), and *d* is the equivalent diameter. The mass transfer coefficient for other flow conditions are given in Ref. 4. From the Chapman-Enskog kinetic theory, the quantity cD_{AB} (in mol cm^{-1} s^{-1}) in Eq. (28) is given by[30]

$$cD_{AB} = 2.2646\times 10^{-5}\,\frac{\sqrt{T\left(\dfrac{1}{M_A}+\dfrac{1}{M_B}\right)}}{\sigma_{AB}^{2}\,\Omega_{AB}}, \tag{29}$$

where T is in K, M is the molecular weight in g mol^{-1} and σ_{AB} is the collision diameter in Å. The collision integral Ω_{AB} is a function of the Lennard-Jones force constant ε_{AB}/κ:[4]

$$\Omega_{AB} = \frac{1}{0.7049 + 0.2910\ln(T\kappa/\varepsilon_{AB})}. \tag{30}$$

The combining laws for the parameters σ_{AB} and ε_{AB}/κ are based on the individual quantities:

$$\sigma_{AB} = \tfrac{1}{2}(\sigma_A + \sigma_B), \tag{31}$$

$$\varepsilon_{AB}/\kappa = \sqrt{(\varepsilon_A/\kappa)(\varepsilon_B/\kappa)}, \tag{32}$$

which can be obtained from Ref. 21 where data exist. Unfortunately, these quantities are not known for many compounds. In this case, within the uncertainty of the present analysis, it can be assumed that $\Omega_{AB} \sim 1$. Furthermore, the collision diameter σ_A (in Å) can be estimated from the liquid molar volume at the normal boiling point V_b (in cm^3 mol^{-1}):[30]

$$\sigma_A = 1.166\,V_b^{1/3}. \tag{33}$$

For a given fission product or actinide compound, V_b can be obtained by a summation of the additive contributions of the individual atoms making up the compound.[31,32,33] For instance, a periodic relation exists where the atomic volume can be correlated with the atomic weight (and to a lesser extent with the periodic grouping, i.e., valence state).[31] Hence, using the structural data of Le Bas as shown in Fig. 1,[31,32] an empirical correlation can be developed as a function of the atomic weight A (g mol^{-1}) for the prediction of the atomic volume contributions ΔV_b (cm^3 mol^{-1}):

$$\Delta V_b = -0.3196\mathrm{A} + 2.734(\ln \mathrm{A})^2 + 8.479\times 10^{-4} A^2. \tag{34}$$

In summary, using the available Le Bas structural data in Table 1, or Eq. (34) for any missing data, V_b can be determined additively for the fission product compound of interest (which exists as either a metal, oxide, hydroxide, etc.) or actinide compound (e.g., UO_3). In turn, σ_A can then be predicted from Eq. (33). This additive methodology yields an average error difference for σ_A of 17% as compared to the measured data in Ref. 21.

2.3.2 Equilibrium partial pressure calculations.

The FACT computer program EQUILIB was used to determine the thermodynamic equilibrium state of the FPs, including a calculation of the partial pressure of the gaseous compounds.[11] In the thermodynamic model, it is implicitly assumed that there is a closed system consisting of both fuel and FPs in a specific proportion, and a gaseous atmosphere of hydrogen/steam at a given system (hydrostatic) pressure and temperature. It is further assumed that all vapor species form an ideal solution. The condensed compounds are considered to be stoichiometric except for the liquid metallic elements which are treated as an ideal solution.

For the CANDU reactor analysis, the FP inventory is assumed to be present in a single fuel channel (13 bundles), as calculated with the ORIGEN code for a Bruce A reactor (with an equilibrium burnup of 100 MWh/kgU) (see Table 2). Within the limitations of the FACT architecture, 23 elements were considered for a given calculation which included: the actinides (U, Np, Pu, Am), FPs (Ce, Y, Te, La, Zr, Ba, Ru, Mo, Pr, Sr, I, Nd, Nb, Cs, Rh, Sb, Eu), and atmospheric constituents (H_2, H_2O).

In order to cover various accident scenarios, the calculations were performed over a wide range of input parameters. The matrix parameters included: (i) temperatures from 1000 to 2000 K (in steps of 50 K) and 2000 to 3000 K (in steps of 100 K); (ii) total system pressure of 1 atm (typical of annealing tests), 3 atm and 10 atm; (iii) hydrogen-to-steam ratios (i.e., H_2/H_2O) of 100 000, 10 000, 1 000, 100, 10, 1, 0.1 and 0.01; and (iv) FP-to-gas atmosphere ratios (i.e., $Cs/(H_2+H_2O)$) of 10^{-6}, 10^{-5} and 10^{-4}. This matrix yields a total of 2232 cases.

The present treatment includes a total of 451 different compounds, with the corresponding distribution of 23 elements over 174 gaseous species and 277 possible condensed phases. The partial pressures of the various FP compounds calculated for each set of conditions of H_2/H_2O ratio and $Cs/(H_2+H_2O)$ ratio can be summed for each of the 4 actinide and 17 FP elements. Several calculations are shown as a function of temperature for various H_2/H_2O and $Cs/(H_2+H_2O)$ ratios in Fig. 2.

2.3.3 Analytical representation: Method of Chemical Potentials (MOCP).

The partial pressure of an individual compound can also be analytically extracted from the FACT analysis in terms of a stand-alone algorithm.[34] For example, for the general reaction for formation of a compound from the elements:

$$xA + yB + zC \overset{K}{\Leftrightarrow} A_xB_yC_z \tag{35}$$

it follows that

$$K = \frac{p_{A_xB_yC_z}}{(p_A)^x(p_B)^y(p_C)^z} = \exp\left(-\frac{\Delta G^o}{RT}\right). \tag{36}$$

Here R is the ideal gas constant, T is the temperature, K is the equilibrium constant for Eq. (35) and ΔG^o is the standard Gibbs energy change of the reaction which can be computed from the standard ("absolute") Gibbs energy equations for the elements and compounds:

$$\Delta G^o = G^o_{A_xB_yC_z} - xG^o_A - yG^o_B - zG^o_C. \tag{37}$$

These ("absolute") Gibbs energy equations represent the combination of enthalpy change (ΔH^o) and absolute entropy (S^o) by the relation

$$G^o = \Delta H^o - TS^o = A + BT + CT^2 + DT^{-1} + ET\ln T + FT^3 + GT^{1/2} + HT^{-2} + I\ln T + JT^4 \tag{38}$$

The apparent mixing of enthalpy change and absolute entropy combines in Eq. (38) to yield the correct ΔG^o for the process in Eq. (35). The use of Eq. (38) is simply a convenience in computing ΔG^o. The coefficients for the Gibbs energy data (for G^o given in J mol^{-1}) in the second relation of Eq. (38) are taken from the FACT database. Equation (36) can therefore be equivalently written as:

$$\log p_{A_xB_yC_z} = x\log p_A + y\log p_B + z\log p_C - \frac{\Delta G^o}{2.303RT}. \tag{39}$$

The partial pressures of individual elemental species i at equilibrium, p_i, (for $i = A, B, C$ ...) can be represented from the FACT results using a Legendre-Fourier series representation for a given H_2/H_2O and $Cs/(H_2+H_2O)$ situation:

$$\log(p_i) = \sum_{m=0}^{11} a_m P_m(T_r), \tag{40}$$

where P_m is a Legendre Polynomial of order m and $T_r = T/3000$. A reduced temperature (T_r) is required so that Eq. (40) is an orthogonal series over the given temperature range. To provide an accurate evaluation of Eq. (40), without the need to carry a large number of significant figures, the Legendre polynomials can be evaluated from the specific values of the two lower-order ones at a given temperature using the recursive relation:[35]

$$P_o = 1,\ P_1 = T_r \text{ and } P_{m+1}(T_r) = \frac{(2m+1)T_rP_m(T_r) - mP_{m-1}(T_r)}{m+1},\ (m = 1,2,...,10). \tag{41}$$

The coefficients (a_m) in Eq. (40) covering the full range of matrix conditions, plus those for the Gibbs energy data of the compounds, total about 18,000. The complete set coefficients are stored in an electronic database form (Microsoft Access program), for efficient use in a computer code,[36] and are available from the authors. Thus, using Eq. (40) for the fitted partial pressure functions of the individual elements, with the Gibbs energy data for Eq. (37), the partial pressures of all the individual compounds can be explicitly recalculated from Eq. (39).[36] On summing the partial pressures for a compound containing a common element i, one also obtains an evaluation of the total elemental partial pressure as depicted in Fig. 2:

$$p^i_{element} = \sum_{\substack{j=compound\\ containing\\ element\, i}} p_j . \tag{42}$$

The average percent difference between FACT and the total pressure reconstitution of Eq. (42) is typically ~3% over the full range of temperature for the 17 FP elements. The inability to refit the data more precisely is due to the change in condensed phase assemblage as temperature alters, which causes small kinks in an otherwise monotonic function (see Fig. 3). Thus, Eqs. (39) and (42) provide a closed-form algorithm to rapidly re-construct the total pressure of an element and all partial pressures of the various compounds containing the element, including the dominant chemical form (i.e., the maximum p_j for a given element i) for a particular reactor accident condition of temperature, H_2/H_2O ratio and $Cs/(H_2+H_2O)$ ratio. The purpose of this procedure is to provide a simple algorithm for compaction of the extensive FACT results with the ability for interpolation over the full range of temperature without the necessity of the time-consuming, Gibbs-energy minimization.[36] The proposed function in Eq. (40) is well-behaved, as shown for example in Fig. 3, and therefore the given algorithm also yields an accurate interpolation between the stated temperatures as compared to actual FACT calculations (see Table 3). This means that the full consideration of the basic premise of low-volatile FP release, based on the assumption of local equilibrium at the point of origin, can be fully explored where the source partial pressure and dominant chemical form of the fission products are quickly retrievable in a more complex model which deals with mass transfer from the source to the environment (see Section 2.3).

3. COMPARISON OF MODEL TO EXPERIMENT

3.1. CRL Experiment Description.

In the CRL experiment (MCE2-T19), the fuel specimen was obtained by cutting a section of a spent element of a Bruce-type design. The fuel fragment was roughly cylindrical in shape (~2.2 mm diameter and 5 mm length), with a weight of 0.200 g and a burnup of 457 MWh/kgU. The sample was introduced into a flowing mixture of argon/2% H_2 (40 ml/min at STP) and ramped in temperature at a rate of ~ 0.15 K/s to 2300 K. After the temperature plateau had been reached, the fuel was exposed to an oxidizing mixture of steam (15 g/h) and argon (40 ml/min at STP) for 7 min. The atmosphere was then replaced by an argon/2% H_2 flow (40 ml/min at STP) and the temperature decreased at the same ramp rate as during the heating period. The oxygen partial pressure of the atmospheric composition was continuously monitored with yttria-stabilized zirconia oxygen sensors at upstream and downstream locations from the fuel specimen.[25] Fission products released from the fuel specimen were swept away such that a gamma-ray spectrometer, collimated at the sample location, provided information on the kinetic release behavior.

3.2 Model Application.

For the given atmospheric and temperature conditions, the model of Eqs. (5), (6), (9), (11) and (12) yields the oxygen partial pressure, hydrogen-to-steam partial pressure ratio and stoichiometry deviation kinetics as shown in Fig. 4.[36] Using the fission-product diffusion model (Section 2.1), the fuel volatilization/matrix stripping model (Section 2.2), the fission-product vaporization model (Section 2.3), and the fission product inventories (N_{go}) of Table 4, the predicted release fractions were calculated for the various release processes (see Table 5).[36] For this analysis, the geometrical surface area $S = 3.46 \times 10^{-5}$ m^2, the effective surface-to-volume ratio $S/V = 5670$ m^{-1}, the grain radius $a = 11.8$ µm, and the equivalent diameter d (i.e., the channel diameter (4.75 mm) – fuel diameter (2.2 mm)) = 2.6 mm. The binary diffusion coefficient required for Eq. (28) was evaluated for the case of a trace fission-product species diffusing in the carrier gas mixture according to the combining law:[4]

$$\frac{1-x_A}{D_{AB}} = \sum_{\substack{j=1\\ j\neq A}}^{n} \frac{x_j}{D_{Aj}}, \tag{43}$$

where j refers to the components of the gas mixture, and x_j and x_A are the mole fractions of the gas components and fission products, respectively. Equation (43) results from the Stefan-Maxwell equations for multi-component diffusion in which the various gas constituents move with the same velocity.[30]

The equilibrium partial pressures (p^{i}_{element}) were derived as described in Section 2.3.3 for the hydrogen-to-steam partial pressure ratio in Fig. 4 and a fixed Cs/(H_2+H_2O+inert) molar ratio. The Cs/(H_2+H_2O+inert) ratio was determined by dividing the "exposed" molar inventory of cesium by the integrated gas flow rate, where the integration starts at a time when the volatile release is first observed to occur. The "exposed" cesium inventory is estimated as the total quantity (N_{go}) in Table 4 times the diffusive release fraction (F_d) in Table 5, i.e., this calculation accounts for the fact that not all of the fission product inventory is in contact with the gas atmosphere, where it is implicitly assumed that all fission product species have roughly the same diffusion coefficient in the fuel matrix.[4] The molar ratio Cs/(H_2+H_2O+inert) is therefore taken as 4.9×10^{-6} for the MCE2-T19 test. Model parameters, representative of the high-temperature plateau region (2300 K) are shown in Table 6, including: the dominant chemical form of the fission-product compound (calculated by MOCP), the liquid molar volume of the fission-product compound (V_b), the collision diameter (σ_A) and Lennard-Jones force constant (ε_A/κ) of the fission-product compound, the binary diffusion coefficient parameter (cD_{AB}), the mass transfer coefficient (k_m) and the total partial pressure of all fission products containing a given element (p^{i}_{element}).

3.3 Discussion.

As shown in Table 5, the overall release fractions (F) that are predicted for most of the observed fission products are in good agreement (typically within a factor of two) with the measured results. The release behaviour of the low-volatile species are controlled by the rate-limiting step of fission-product vaporization from the fuel surface (F_v). On the other hand, the release behaviour of the more volatile species (e.g., cesium) are determined by the slower matrix diffusion step (F_d). The release fractions for the various release mechanisms were evaluated at each time step of ~ 1 min, in which the corresponding rate-limiting step was determined.[36]

The measured release fractions of ^{144}Ce and ^{106}Ru have been inferred from the release behaviour of their short-lived daughter products (^{144}Pr and ^{106}Rh). Due to the very short half-life of 29.8 s for ^{106}Rh, the measured release fraction of this isotope is directly indicative of the parent fraction. No significant release of ^{144}Pr (half-life of 17.3 min) was observed within the measurement uncertainty up to the end of the high-temperature steam period. Consequently, it is believed that the cumulative release of this isotope is attributable solely to the release of its parent (which would therefore affect the parent-daughter equilibrium). However, if some release of ^{144}Pr did in fact occur, the stated value in Table 5 would be an overestimate of the measured release of ^{144}Ce (i.e., some release of ^{144}Pr is expected on thermodynamic grounds as a consequence of a finite partial pressure for this species). In this case, the model prediction would be in better agreement with experiment.

The europium release is overestimated where a hydroxide compound (EuOH) predominates in Table 6. In fact, the original thermodynamic data of Ref. 21 yielded an unrealistically high vapor pressure for the europium hydroxide compounds, EuOH and $Eu(OH)_2$. The thermodynamic data from the Victoria code[21] for these compounds are not consistent with the enthalpy change and absolute entropy data for the hydroxides of the other lanthanide series elements taken from Cubicciotti.[6] Instead, a new set of thermodynamic quantities were estimated for the europium hydroxides for use in the present FACT analysis, based on an extrapolation of the trends in the lanthanide series data. However, this extrapolated set still results in an overprediction of the partial pressure for europium, as shown in Table 5, indicating a need for better thermochemical data for the hydroxide forms of europium.

In the MCE2-T19 test, which was conducted in steam, significant fuel volatilization occurred. The fuel volatilization fraction predicted with the thermodynamic/mass transfer model of Section 2.2 (i.e., $F_{\mathrm{vol}} = 70\%$ in Table 5) was in excellent agreement with observation, as inferred from the measured pre- and post-test sample masses, i.e., $\Delta m/m = (0.200 - 0.046\ \mathrm{g})/(0.200\ \mathrm{g}) \sim 77\%$.

The fuel volatilization model can also be compared to that developed in Ref. 9. For instance, Eqs. (18), (28) and (29) predict for the fuel volatilization rate a dependency on temperature and system pressure of $T^{1/2}$ and p_{tot}^{-1}, whereas the Alexander and Ogden model yield a quite different result of $T^{1.25}$ and $p_{\mathrm{tot}}^{-2/3}$. This difference arises because of the questionable assumption of effusive flow (i.e., a Knudsen relation) in the Alexander and Ogden model for the calculation of the sublimation flux of the UO_3 vapor. On the other hand, the model of Section 2.2 is self-consistent with the formalism for fission product vaporization (Section 2.3) and is in excellent agreement with the CRL test results. In addition, contrary to the Alexander and Ogden model, no adjustable constants have been used, i.e., the present model is based on thermochemical data and a well established heat (mass) transfer coefficient (for annular flow).

4. CONCLUSIONS

A model has been developed to describe the release behaviour of low-volatile fission products from uranium dioxide fuel during severe CANDU reactor accident conditions. The vaporization model is based on the equilibrium partial pressures of the fission products and mass transport theory. The equilibrium partial pressures were determined by Gibbs-energy minimization with the FACT thermodynamics package for a system consisting of a condensed phase (UO_2 plus fission products) and a gas phase (H_2O and H_2 plus gaseous fission products). The extensive FACT results were recast into an analytical form, using the method of chemical potentials, for model implementation into a stand-alone computer code.

A theoretical treatment has also been used to describe the effect of fuel volatilization on the fission-product release behaviour. The model includes the effects of the fuel oxidation kinetics on the production of UO_3 vapor and the subsequent mass transfer of this gaseous phase through a boundary layer at the surface of the fuel. This matrix-stripping process competes with that of solid-state diffusion as a mechanism of fission-product release to the fuel surface.

The model is in good agreement with the fission-product release data obtained in the CRL test, MCE2-T19, performed with a fuel-fragment specimen at 2300 K in steam. This model is also able to predict the observed fuel volatilization in the CRL test.

ACKNOWLEDGEMENTS

The present analysis was supported by the Natural Sciences and Engineering Research Council of Canada (award no. OGP0155726). The CRL experiment was supported by Atomic Energy of Canada Limited, Ontario Hydro, Hydro Quebec and New Brunswick Electric Power Corporation under the Candu Owners Goup agreement.

REFERENCES

1. M.F. OSBORNE and R.A. LORENZ, "ORNL Studies of Fission Product Release Under LWR Severe Accident Conditions," Nucl. Safety, 33, 344 (1992).
2. B.J. LEWIS, B. ANDRE, B. MOREL, P. DEHAUDT, D. MARO, P.L. PURDY, D.S. COX, F.C. IGLESIAS, M.F. OSBORNE and R.A. LORENZ, "Modelling the Release Behaviour of Cesium During Severe Fuel Degradation," J. Nucl. Mater., **227**, 83 (1995).
3. A.B. REYNOLDS, J.L. KELLY and S.T. KIM, "Role of Surface Vaporization in Low-Volatility Fission Product Release Experiments," Nucl. Technol., **74**, 76 (1986).
4. B.J. LEWIS, B. ANDRE, G. DUCROS and D. MARO, "A Model for Nonvolatile Fission Product Release During Reactor Accident Conditions," Nucl. Technol., **116**, 34 (1996).
5. D. CUBICCIOTTI, "Vaporization Thermodynamics of Fission Products from Fuel Under Nuclear-Accident Conditions," Advances in Ceramics, Vol. 17, p. 211, American Ceramic Society, Columbus, Ohio, 1986.
6. D. CUBICCIOTTI, "Vapor Transport of Fission Products Under Nuclear Accident Conditions," J. Nucl. Mater. **154**, 53, (1988).
7. D. CUBICCIOTTI and B.R. SEHGAL, "Vapor Transport of Fission Products in Postulated Severe Light Water Reactor Accidents," Nucl. Technol., **65**, 267 (1984).

8. C.A. ALEXANDER, J.S. OGDEN, L. CHAN and R.W. WRIGHT, "Matrix Stripping and Fission Product Release at High Temperatures," Proceedings International Symposium on Severe Accidents in Nuclear Power Plants, Sorrento, Italy, March 21-25, 1988, IAEA-SM-296/99, International Atomic Energy Agency (1988).
9. C.A. ALEXANDER and J.S. OGDEN, "Vaporization of UO_2 at High Temperatures and High Pressures: A Generic Relation for Volatilization," High Temp. - High Pressures, **21**, 149 (1990).
10. D.S. COX, C.E.L. HUNT, Z. LIU, F.C. IGLESIAS, N.A. KELLER, R.D. BARRAND and R.F. O'CONNOR, "A Model for the Release of Low-Volatility Fission Products in Oxidizing Conditions," Proceedings of the 12th Annual Conference of the Canadian Nuclear Society, Saskatoon, Saskatchewan, Canada, June 9-12, 1991, AECL-10440, Atomic Energy of Canada Limited.
11. C.W. BALE, A.D. PELTON and W.T. THOMPSON, "Facility for the Analysis of the Chemical Thermodynamics," McGill University and École Polytechnique, 1995.
12. D.R. STULL and H. PROPHET, JANAF Thermochemical Tables, second edition, National Standard Reference Data System, NSRDS-NBS 37, U.S. Department of Commerce, National Bureau of Standards, Washington, D.C., June 1971 (and updates).
13. I. BARIN and O. KNACKE, Thermochemical Properties of Inorganic Substances, Springer-Verlag Berlin Heidelberg, New York, 1973.
14. I. BARIN, O. KNACKE and O. KUBASCHEWSKI, Thermochemical Properties of Inorganic Substances, Supplement, Springer-Verlag Berlin Heidelberg, New York, 1977.
15. E.H.P. CORDFUNKE and R.J.M. KONINGS, Thermochemical Data for Reactor Materials and Fission Products, North Holland, Elsevier Science Publishers B.V., Amsterdam, 1990.
16. F. GARISTO, "Thermodynamic Behaviour of Ruthenium at High Temperatures," Atomic Energy of Canada Limited, AECL-9552, (1988).
17. T.B. LINDEMER, T.M. BESMANN and C.E. JOHNSON, "Thermodynamic Review and Calculations - Alkali-Metal Oxide Systems with Nuclear Fuels, Fission Products, and Structural Materials," J. Nucl. Mater. **100**, 178 (1981).
18. S. DASH, Z. SINGH, R. PRASAD and D.D. SOOD, "The Standard Molar Gibbs Energy of Formation of $BaMoO_3(s)$," J. Nucl. Mater. **207**, 350 (1993).
19. R. SAHA, R. BABU, K. NAGARAJAN and C.K. MATHEWS, "Thermodynamic Properties of Ternary Oxides of Fission Products from Calorimetric Measurements," J. Nucl. Mater. **167**, 271 (1989).
20. H. KLEYKAMP, "Constitution and Thermodynamics of the Mo-Ru, Mo-Pd, Ru-Pd and Mo-Ru-Pd Systems," J. Nucl. Mater. **167**, 49 (1989).
21. T.J. HEAMES, D.A. WILLIAMS, N.E. BIXLER, A.J. GRIMLEY, C.J. WHEATLEY, N.A. JOHNS, P. DOMAGALA, L.W. DICKSON, C.A. ALEXANDER, I. OSBORN-LEE, S. ZAWADZKI, J. REST, A. MASON and R.Y. LEE, "VICTORIA: A Mechanistic Model of Radionuclide Behavior in the Reactor Coolant System Under Severe Accident Conditions," U.S. Nuclear Regulatory Commission, NUREG/CR-5545, SAND90-0756, Rev. 1, R3, R4, December 1992.
22. B.J. LEWIS, B.J. CORSE, W.T. THOMPSON, M.H. KAYE, F.C. IGLESIAS, P. ELDER, R. DICKSON and Z. LIU, "Low Volatile Fission Product Release and Fuel Volatilization During Sever Reactor Accident Conditions," submitted to J. Nucl. Mater.
23. P. PURDY, "A Model for Fuel Oxidation and Diffusion-Based Fission Product Release Under Severe Nuclear Reactor Accident Conditions," Master of Science (Engineering) Dissertation, Department of Physics, Queen's University, 1995.
24. P.E. BLACKBURN, "Oxygen Pressures over Fast Breeder Reactor Fuel, (I) A Model for $UO_{2\pm x}$," J. Nucl. Mater. **46**, 244 (1973).
25. D.S. COX, R.F. O'CONNOR and W.W. SMELTZER, "Measurement of Oxidation/Reduction Kinetics to 2100°C Using Non-Contact Solid-State Electrolytes," Solid-State Ionics, **53-56**, 238 (1992).
26. A.C. BRITO, F.C. IGLESIAS, Y. LIU, C.J. WESTBYE, D.S. COX and B.J. LEWIS, "Modelling of UO_2 Oxidation In Steam," Proceedings of the 17th Annual Conference of the Canadian Nuclear Society, Fredericton, New Brunswick, Canada, June 9-12, 1996, C.2, Canadian Nuclear Society, 1996.
27. O. KUBASCHEWSKI and C.B. ALCOCK, Metallurgical Thermochemistry, 5th Ed., Pergamon Press, New York, 1979.

28. R.J. ACKERMANN and A.T. CHANG, "Thermodynamic Characterization of the U_3O_{8-z} Phase," J. Chem. Thermodynamics, **5**, 873 (1973).
29. D.S. COX, "FOXSIM Version 2: Fuel Oxidation Simulation for UO_2 in Air and Steam," Atomic Energy of Canada Limited, Internal Report RC-402, February 1990.
30. R.B. BIRD, W.E. STEWART and E.N. LIGHTFOOT, Transport Phenomena, John Wiley & Sons, New York (1960).
31. G. LE BAS, The Molecular Volumes of Liquid Chemical Compounds, Longmans, Green and Co., London, 1915.
32. R.H. PERRY and C.H. CHILTON, Chemical Engineers' Handbook, 5th ed., McGraw-Hill Book Co., New York, 1973, p. 3-229.
33. R.C. REID, J.M. PRAUSNITZ and B.E. POLING, The Properties of Gases and Liquids, 4th ed., McGraw-Hill Book Co., New York, 1987.
34. M.H. KAYE, B.J. LEWIS, W.T. THOMPSON and F.C. IGLESIAS, "Oxidation of Nuclear Fuel Rods During a Loss-of-Coolant Accident," 8th Canadian Materials Science Conference, London, Ontario, June 11-14, 1996.
35. M.R. SPIEGEL, Mathematical Handbook of Formulas and Tables, Schaum's Outline Series, McGraw-Hill Inc., New York, 1968, p. 147.
36. B. CORSE, "FORM 2.0: Fuel Oxidation and Release Model, A Computer Code to Predict Low-Volatile Fission Product Release and Fuel Volatilization From Uranium Dioxide Fuel During Severe Reactor Accident Conditions," Master of Engineering Dissertation, Department of Chemistry and Chemical Engineering, Royal Military College of Canada, 1997.

TABLE 1: VOLUME INCREMENTS FOR THE CALCULATION OF MOLAR VOLUMES

Element	Le Bas Atomic Volume Increment, ΔV_b (cm^3 mol^{-1})
As	30.5
Br	27.0
I	37.0
Sb	34.2
Sn	42.3
H	3.7
O	7.4 (12.0 in acids)

TABLE 2: MOLES OF ACTINIDES AND FISSION PRODUCT ELEMENTS USED IN THE FACT ANALYSIS

Actinides	Moles	Fission Products	Moles	Fission Products	Moles
Uranium (a)	1015	Cerium	0.824	Strontium	0.421
Neptunium	0.096	Yttrium	0.215	Iodine	0.077
Plutonium	2.754	Tellurium	0.138	Neodymium	0.859
Americium	0.0064	Lanthanum	0.332	Niobium	0.043
		Zirconium	1.442	Cesium	0.745
		Barium	0.389	Rhodium	0.166
		Ruthenium	0.899	Antimony	0.006
		Molybdenum	1.150	Europium	0.025
		Praseodymium	0.265		

(a) Assumed chemical form for FACT analysis is UO_2.

TABLE 3: COMPARISON OF MOCP (INTERPOLATED) WITH FACT CALCULATIONS(a)

Temperature (K)	Vapor Pressure of BaMoO4 (atm)		Δ%
	FACT	MOCP	
1225	2.86×10^{-13}	2.60×10^{-13}	9.2
1725	4.17×10^{-8}	4.39×10^{-8}	-5.1
2250	3.25×10^{-6}	3.61×10^{-6}	-11.0
2750	3.84×10^{-7}	4.27×10^{-7}	-11.3

(a) For $H_2/H_2O = 1$ and $Cs/(H_2+H_2O) = 10^{-4}$.

TABLE 4: INITIAL FISSION PRODUCT INVENTORIES IN THE MCE2-T19 TEST

Element	Inventory, N_{go} (atom)	Element	Inventory, N_{go} (atom)
Cerium	8.17×10^{17}	Praseodymium	3.28×10^{17}
Cesium	8.71×10^{17}	Rhodium	2.39×10^{17}
Europium	4.52×10^{16}	Ruthenium	1.14×10^{18}
Niobium	1.61×10^{16}	Zirconium	1.56×10^{18}

TABLE 5: COMPARISON BETWEEN MEASURED AND PREDICTED RELEASE FRACTIONS

Chemical Species (Isotope)	Fractional Release (%)					
	Predicted(a)					Measured
	RLS	F_d	F_{vol}	F_v	F	F
Ce (144)	V	96	70	4.6	5	~25(b)
Cs (137)	D/MS	96	70	100	99	98
Eu (154)	D/MS	96	70	100	99	0
Nb (95)	D/MS	96	70	100	99	46
Ru (106)	V	96	70	39	39	81(b)
Zr (95)	V	96	70	0.08	0.08	0

(a) RLS = rate-limiting step (V = Vaporization, D = Diffusion, MS = Matrix Stripping); F_d = diffusion release fraction (all species are assumed to have the same diffusion coefficient as cesium); F_{vol} = fuel volatilization release fraction (the matrix stripping release fraction is assumed to be the same as the volatilization release fraction); F_v = fission-product vaporization release fraction; F = overall release fraction.

(b) Inferred from the release behaviour of the daughter isotopes ^{144}Pr and ^{106}Rh.

TABLE 6: CALCULATION OF VAPORIZATION MODEL PARAMETERS FOR THE MCE2-T19 TEST(a)

Fission Product				Combined Quantities		Total Element Vapor Pressure
Dominant Compound	Liquid Molar Volume, V_b (cm^3 mol^{-1})	Collision Diameter, σ_A (Å)	Lennard-Jones Force Constant, ε_A/κ (K)	Binary Diffusivity, cD_{AB} ($\times 10^{-3}$ mol m^{-1} s^{-1})	Mass Transfer Coefficient, k_m (mol m^{-2} s^{-1})	$p^{i}_{element}$ (atm)
CeO	46.1	4.18	(b)	2.66	4.17	3.03×10^{-7}
CsOH	49.2	4.08	1046	2.96	4.64	4.70×10^{-6}
EuOH	51.1	4.33	(b)	2.33	3.66	1.84×10^{-7}
NbO_2	48.6	4.25	(b)	2.64	4.14	1.94×10^{-7}
RuOH	45.7	4.17	(b)	2.71	4.26	3.86×10^{-6}
ZrO_2	48.4	3.21	10146	2.90	4.55	1.51×10^{-8}

(a) The parameters correspond to the high-temperature plateau at 2300 K.

(b) Not available. Since this parameter is needed for the calculation of Ω, it is therefore assumed that Ω is approximately unity.

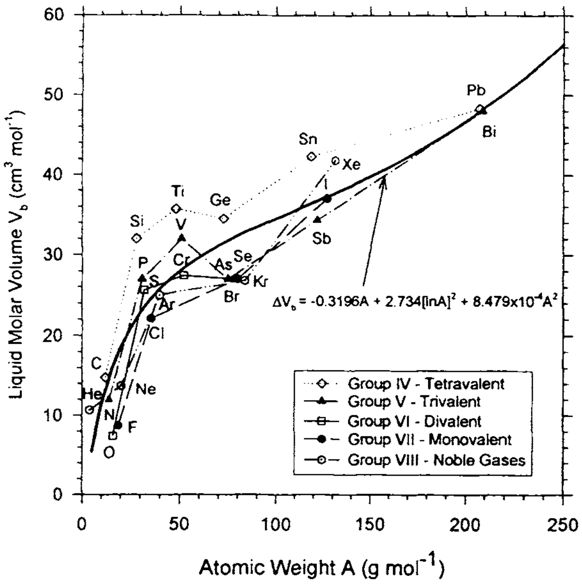

FIG. 1. RELATION BETWEEN LE BAS VOLUMES AND ATOMIC WEIGHTS.

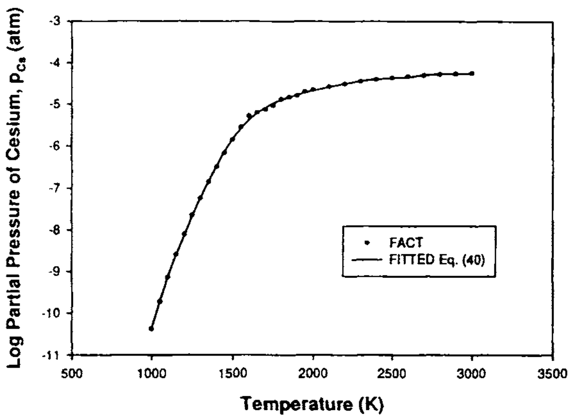

FIG. 3. EXAMPLE OF THE FITTING OF EQ. (40) FOR THE CS PARTIAL PRESSURE TO ACTUAL FACT CALCULATIONS AS A FUNCTION OF TEMPERATURE, WITH $H_2/H_2O=1$ AND $CS/(H_2+H_2O)=10^{-4}$.

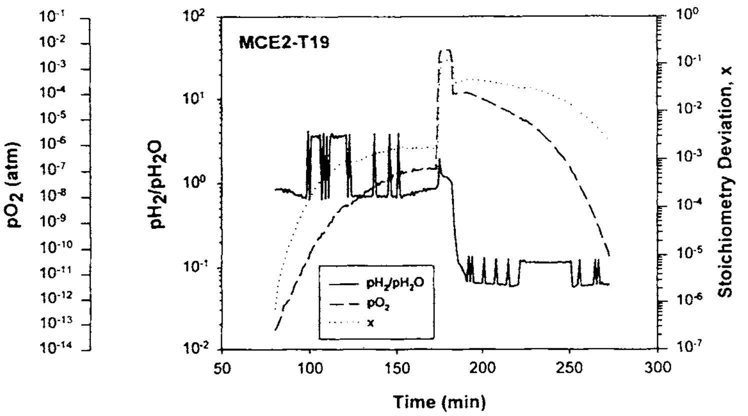

FIG. 4. OXYGEN PARTIAL PRESSURE, H_2/H_2O PARTIAL PRESSURE RATIO AND STOICHIOMETRY DEVIATION HISTORIES FOR THE MCE2-T19 TEST.

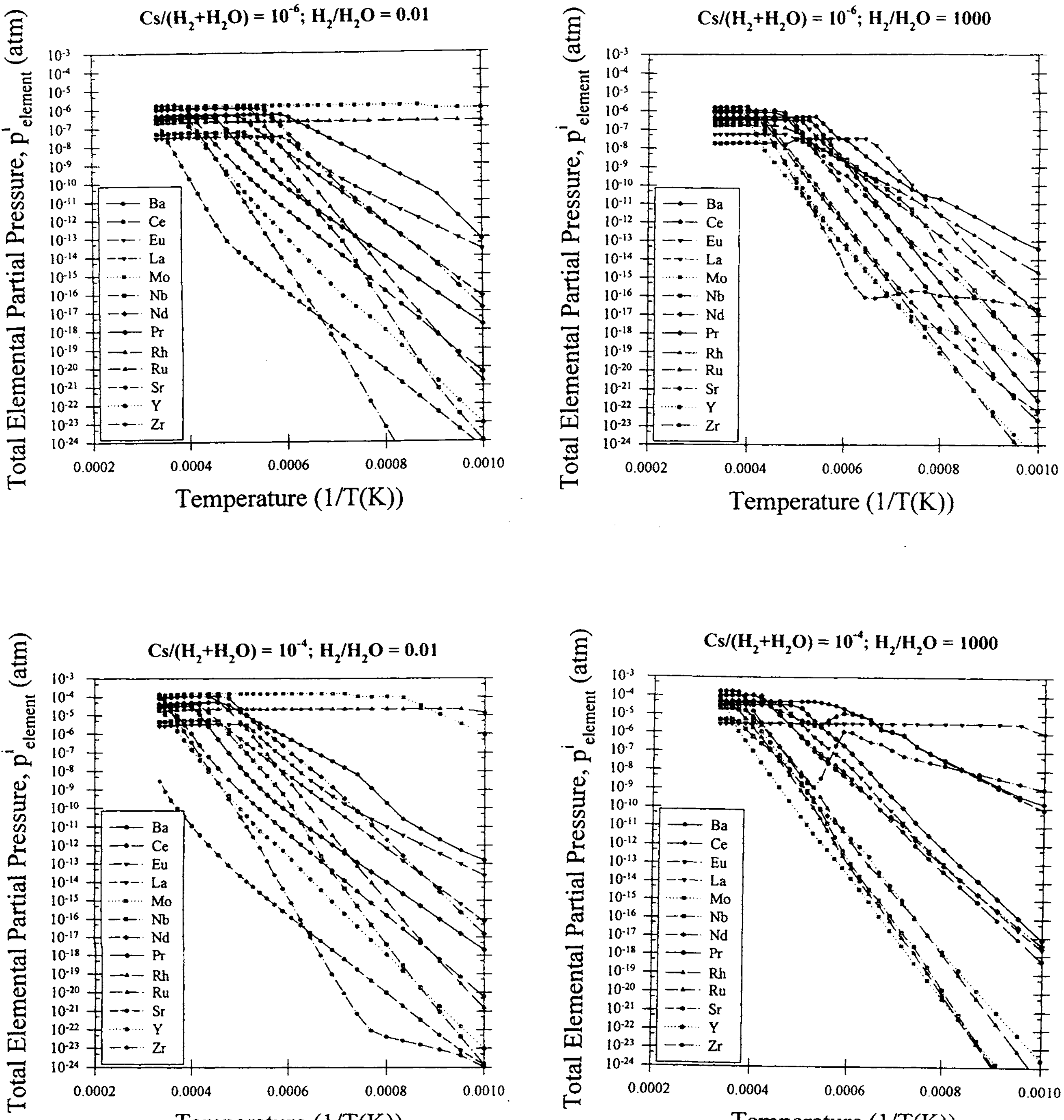

FIG. 2. TOTAL ELEMENTAL PARTIAL PRESSURE VERSUS TEMPERATURE FOR LOW-VOLATILE FISSION PRODUCTS AT A TOTAL SYSTEM PRESSURE OF 1ATM.